Scripta Materialia 116 (2016) 117–121

Contents lists available at ScienceDirect

Scripta Materialia

journal homepage: www.elsevier.com/locate/scriptamat

Block and sub-block boundary strengthening in lath martensite

C. Du, J.P.M. Hoefnagels *, R. Vaes, M.G.D. Geers

Department of Mechanical Engineering, Eindhoven University of Technology, P.O. Box 513, 5600 MB Eindhoven, The Netherlands

ARTICLE INFO

Article history:
Received 25 November 2015
Received in revised form 28 January 2016
Accepted 29 January 2016
Available online xxxx

Keywords:
Lath martensite
Boundaries
Strengthening mechanism
Uniaxial micro-tensile test

ABSTRACT

Well-defined uniaxial micro-tensile tests were performed on lath martensite single block specimens and multi-block specimens with different numbers of block boundaries parallel to the loading direction. Detailed slip trace analyses consistently revealed that the {110}<111> slip system with the highest Schmid factor is activated. Both block and sub-block boundaries act as barriers to dislocation motion, whereby a Hall–Petch like behavior is observed. Sub-block boundary strengthening appears to be only slightly less effective than block boundary strengthening, even though fracture analyses indicate that dislocation motion can cross sub-block boundaries, but not block boundaries.

© 2016 Elsevier Ltd. All rights reserved.

Lath martensite, the most typical morphology of martensite, has high industrial relevance being the prime constituent that elevates the strength in high strength steels, such as dual-phase steel, transformation-induced plasticity steel and quenching-partitioning steel. For decades, research has been conducted on the strengthening mechanisms of this material, which can be categorized into (i) forest dislocation hardening [1,2], (ii) solid solution hardening by alloying elements [2], (iii) precipitation strengthening, e.g., by carbides [2,3], and most importantly (iv) substructure boundary strengthening [4–11]. Indeed, the hierarchical structure, which shows substructures of packets, blocks and sub-blocks within prior austenite grains, gives lath martensite an abundance of internal boundaries [12]. It was suggested that these boundaries can act as potential barriers to dislocation motion [2,4,5,6].

The mechanical effect of lath martensite boundaries has been investigated in a number of high quality research studies, which can be categorized according to the experimental methodologies used: Morito et al. and Zhang et al. performed macroscopic tensile tests and concluded that a Hall–Petch relation holds between the yield strength and the averaged block size [4,5]. A more microscopic analysis was carried out by Ohmura et al. through nano- and micro-indentation tests, who concluded that the block structure increases the hardness of martensite [3,6], although no differentiation was made between different types of (packet/block/sub-block) boundaries. Shibata et al. [7,8] performed micro-bending tests, including two single-block specimen tests. From slip trace analysis from the bending side, where the slip activity is highly inhomogeneous due to the complex loading state, they concluded that the block boundaries are the most effective barriers to dislocation motion. The influence of the sub-block boundaries' presence was, however, not investigated in detail. Alternatively, lath martensite has been tested by micro-pillar compression tests, including TEM diffraction analysis, by Ghassemi-Armaki et al. [9,10], who found that single block specimens show perfect elasto-plastic behavior, whereas multiple block specimens show significant strain hardening. These authors acknowledge, however, that the multiple-block specimens may be jeopardized with one or more packet boundaries, making it difficult to determine whether the hardening is due to the block or packet boundaries. Finally, micro-tension tests on lath martensite, including (single-sided) electron-backscattered diffraction (EBSD) analysis, were conducted by Mine et al. [11]. Besides specimens containing multiple packets and even multiple prior austenite grains, also two single-packet specimens were tested with the block boundaries parallel to the loading direction. The authors concluded that block boundaries can be an effective strengthening mechanism, although the contribution of the sub-block boundaries was again not studied. In general, the distinct role of block and sub-block boundaries in terms of the resulting strengthening mechanism remains to be unclear. Therefore, to directly expose the most relevant microscopic deformation mechanisms, reliable experiments under well-defined loading conditions are required, testing single-packet specimens with different numbers of block boundaries as well as single-block specimens with different numbers of sub-block boundaries. The mechanical tests should be accompanied by detailed orientation analyses from at least two sides to confirm the 3D orientation(s) throughout the specimen volume.

In this study, we perform uniaxial micro-tensile tests, using an in-house developed nano-force tensile tester (Fig. 1(a, b)) [13], of lath martensite specimens consisting of either a single packet or a single block with a range of block or sub-block boundaries respectively. The

* Corresponding author.
E-mail address: j.p.m.hoefnagels@tue.nl (J.P.M. Hoefnagels).

http://dx.doi.org/10.1016/j.scriptamat.2016.01.043
1359-6462/© 2016 Elsevier Ltd. All rights reserved.

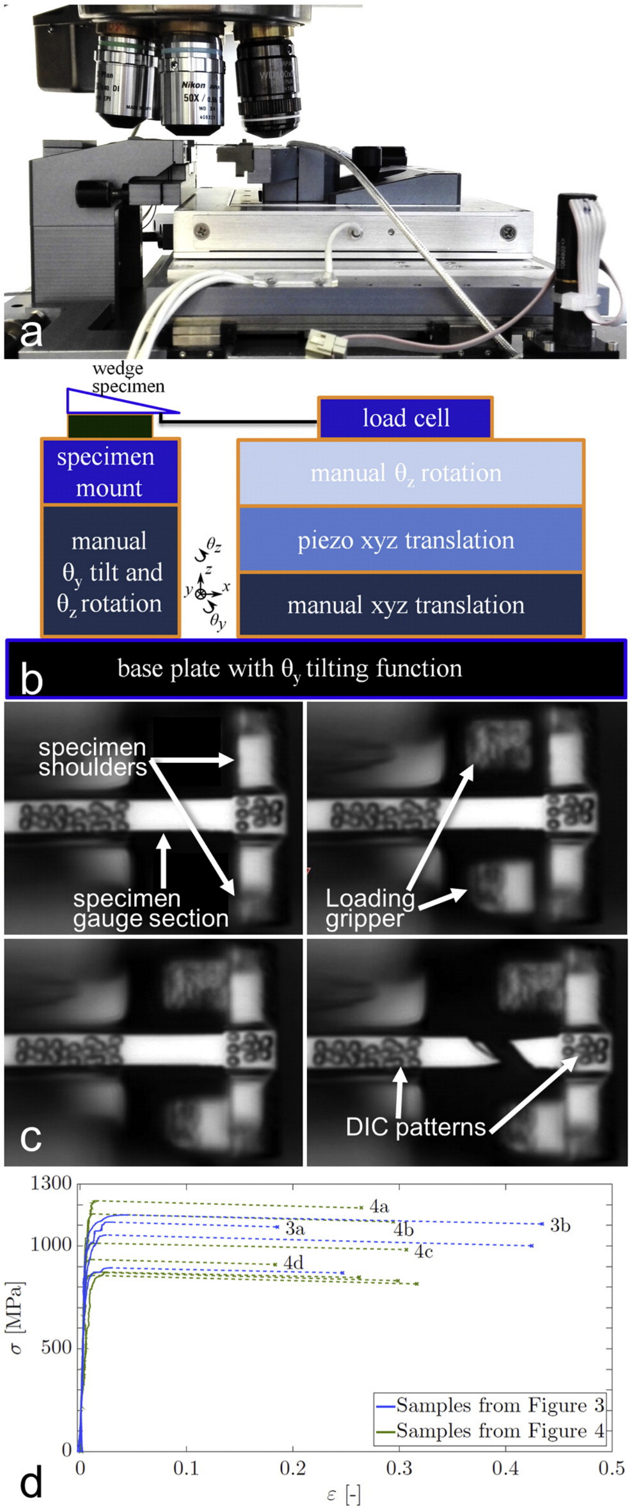

Fig. 1. (a) The in-house developed nano-force tensile stage under an optical profilometer. (b) Schematic drawing of the tensile stage. (c) The testing procedure, in which the load is applied by a 'double-hook' gripper on the specimen shoulders (only the specimen gauge section is in focus). (d) Stress–strain curves of all specimens shown in Figs. 3 and 4; the specimens discussed in detail are labeled with their figure numbers. Note that in the unstable deformation regime (dashed line) the applied load decreases slightly.

methodology involves the following steps: (i) fabrication of a wedge of lath martensite by grinding/polishing/electro-chemical etching, (ii) careful selection of the specimen location at the edge of wedge based on EBSD maps, (iii) focused ion beam milling of micro-tensile specimens with constant thickness, (iv) detailed top- and bottom-side EBSD analysis of each specimen (Figs. 2, 3, 4), (v) uniaxial tensile tests with highly accurate specimen alignment, force- and displacement measurements (Fig. 1(a, b, c)) under (vi) in-situ optical microscopy enabling microscopic slip trace analysis [14]. We will show that not only block boundaries but also sub-block boundaries play a key role in lath martensite strengthening.

Bulk lath martensite (0.092C–1.68Mn–0.24Si–0.57Cr) out of which the micro-tensile specimens are made was heat treated by homogenization at austenite temperature (first batch, 950 °C for 30 min; second batch, 1000 °C for 120 min), followed by water quenching. Most specimens were discarded for analysis because detailed EBSD analysis at both specimen sides showed that the microstructure was not homogeneous over the thickness. For a first batch of specimens, with an average block size smaller than the specimen size, only one specimen was identified with the intended microstructure and desired orientation. Therefore, a second batch of specimens with larger block size was produced with more suitable specimens. The single specimen retained from the first batch is first discussed, since it clearly reveals the role of the block boundary, see Fig. 2.

The EBSD maps of the top and bottom sides (Fig. 2(a, b)) confirm that the block boundary is approximately in the middle of the specimen and runs vertically through the thickness. The pole figures of the top and bottom sides are shown in Fig. 2(e, f), which demonstrate the uniformity of the microstructure within the specimens. The block boundary was confirmed to be a high angle boundary with ~60 degree misorientation. From the austenite-to-martensite orientation relationship it is known that boundaries inside packets form at a {111} prior austenite plane, i.e. parallel to a {110} martensite plane, therefore, the dots (red circles) on the peripheral in the {110} plots in Fig. 2(e, f) confirm that the block boundary is perpendicular to the specimen surface. Black circles highlight the favorable slip direction and slip plane of the {110}<111> slip systems. The marked slip traces (dotted lines) in Fig. 2(d) is in good agreement with the favorable slip systems, considering the significant crystal rotation upon fracture. More convincing evidence for single slip system activation is shown below for the single block specimens. Interestingly, the fracture surfaces join exactly at the block boundary in the middle, where the slip systems are interrupted. This is the first direct evidence that block boundaries in lath martensite act as barriers to dislocation motion for the case where the activated slip system is crossed by a block boundary.

From the second batch of specimens, a series of specimens with different configurations of boundaries are produced and tested: specimens with no block boundaries (i.e. single block specimens), 1 parallel block boundary and multiple parallel block boundaries. In Fig. 3(a, b), two examples of specimens with multiple block boundaries are shown. In the case of few block boundaries (Fig. 3(a)), with large boundary-free regions at the specimen sides, the fracture propagates from both specimen sides and arrests at the first block boundary, similar to the single block boundary case. However, between the two block boundaries, the slip activity is more complex due to the induced loading constraints, resulting in a jagged fracture surface. The same phenomenon is also observed when the boundary-free regions at the specimen sides are small, due to the presence of many block boundaries (Fig.3(b)). Due to the fact that the dislocations cannot propagate through block boundaries, a zig-zag fracture surface is formed with multiple peaks, again in agreement with the block boundaries. The identified slip systems of both samples are in line with the ones marked with corresponding colors of the blocks in the pole figures (Fig. 3(c, d)).

To analyze the strengthening caused by block boundaries, Fig. 3(e) shows the critical stress, $\tau_{critical}$, versus the square root of the average number of block boundaries, $\sqrt{m}$ where m is the average number of block boundaries observed at both sides. $\tau_{critical}$ is calculated by multiplying the highest Schmid factor of the largest block with the tensile strength, which is used as some specimens localize before 2% strain offset.

Download English Version:

https://daneshyari.com/en/article/7912277

Download Persian Version:

https://daneshyari.com/article/7912277

Daneshyari.com